12th IEA Heat Pump Conference 2017

MODEL PREDICTIVE HEAT PUMP- AND BUILDING CONTROL TO MAXIMIZE PV-POWER ON SITE USE

Martin Felix Pichler[a,*], Andreas Heinz[a], René Rieberer[a]

[a]Graz University of Technology Institute of Thermal Engineering, Inffeldgasse 25/B, 8010 Graz, Austria

Abstract

Grid-connected photovoltaic (PV) power plants may lead to unwanted disturbance to the electricity grid. In addition, low feed-in tariffs motivate a homeowner and operator of the PV plant to maximize the electricity self-consumption. Thermal storage capacity enables to maximize the utilization of PV-power to pre- or "overheat" a water tank or the whole building, and avoid grid-overcharge and unwanted disturbances at the same time.

A PV system in connection with a speed-controlled compression heat pump (HP) for domestic hot water (DHW) and space heating (SH) purposes of a single family house (SFH) poses a challenging control task in this context. A model predictive controller provides a suitable approach to such a task with partly conflicting control objectives.

This research investigates a HP-PV system for Central Europe, consisting of a small-scale grid connected PV plant in connection with a HP charging a thermal storage and supplying the energy for space heating. The manuscript describes the reference system and explains the control task. The results for a single family house with a heating demand of ~45 kWh/(m^2 a) and 20 m^2 of south oriented PV modules indicate a share of 50% of the generated PV being directly used by the HP. During the heating season from September to April, this share is 77%. With respect to the total HP electricity consumption the average annual grid-consumption may be reduced to 40%.

© 2017 Stichting HPC 2017.
Selection and/or peer-review under responsibility of the organizers of the 12th IEA Heat Pump Conference 2017.

Keywords: PV, load change flexibility, smart control, MPC, thermal storage, HP.

* Corresponding author. Tel.: +43 316 873 7312; fax: +43 316 873 7305.
E-mail address: martin.pichler@tugraz.at or martin.pichler@gmx.eu.

Nomenclature

Symbol	Explanation	Unit
DHW	Domestic hot water demand	kWh/a
MPC	Modell predictive controller	
P_{comp}	Compressor power consumption	kW
P_{PV}	Generated PV-power	kW
Q_{SH}	Required energy for space heating (SH)	kWh
$\dot{Q}_{cond}, \dot{Q}_{desup}$	Thermal output of condenser, desuperheater	kW
$Q_{evap,brine}$	Consumed energy from the ground	kWh
$Q_{HP,loss}$	Start-, Stop-, and thermal HP losses	kWh
$Q_{pipe,loss}$	Pipe losses	kWh
$Q_{TES,loss}$	TES losses against an ambient temperature of 20 °C	kWh
$Q_{TES,DHW}$	TES energy required for DHW heating	kWh
SH	Space heating	
TABS,TES	Thermally activated building system, thermal energy storage	
W_{PV}	PV generated energy	kWh
$W_{PV,grid}$	PV generated energy fed into the grid	kWh
$W_{HP,PV}$	Directly consumed PV-generated energy	kWh
W_{HP}	Total electricity demand oft the HP	kWh
W_{grid}	Electricity consumed from the grid	kWh
$\vartheta_{air}, \vartheta_{op}$	Room air-, operative room temperature	°C
$\vartheta_{oa}, \vartheta_{grd}$	Outside ambient-, ground temperature	°C
$\vartheta_{co}, \vartheta_{ci}$	Condenser outlet and inlet temperature (water)	°C
ϑ_{do}	Desuperheater outlet temperature (water)	°C
ϑ_{TES}	Water temperature in the upper part of the TES	°C

1. Introduction

The end-consumer electricity price in Austria is approximately 20 cent/kWh. However, the grid feed-in remuneration for household generated photovoltaic (PV) energy is only 6 cent/kWh. In addition, with total actual costs of approximately 14 cent/kWh, grid parity is achieved for PV generation; i.e. the costs of local PV generation are already smaller or equal the prices that end-consumers have to pay for electricity, compare [1]. The low feed-in remuneration limits the incentives for further PV installations by end-consumers. Grid parity on the other hand poses a motivation for further PV installations, but end-consumers may only make use of this advantage through PV self-consumption. This is one main motivation for the presented research. By nature, renewable sources such as the sun or the wind are volatile, which causes a number of disadvantages from a grid operator's point of view. Grid congestion is one major disadvantage. This congestion may be avoided through extensive exploitation of e.g. PV self-consumption or any other type of PV-led device operation. The PV-led device operation or maximization of PV self-consumption poses the prototypical control task, elaborated and presented in this work.

Dynamic fossil-fueled electric generators, compensating for variable grid demand or assisting volatile renewable sources, go against the trend of becoming independent of this source. An alternative approach represents demand-side management (DSM). DSM describes the voluntary and timely adjustment of a given load [2]. Characterized by the imagination of a peak and valley shaped load profile three types are distinguished: reduction- (peak clipping), increase- (valley filling) and shifting- (load shifting) of consumption. That is, rather than providing any existing demand, DSM strives to shape the demand to fit the current supply. This is especially interesting in connection with volatile renewable energy sources. The approach presented in this paper refers also to load shifting.

The aim is to maximize rather than curtail energy generation from renewable sources. This motivates the search for applications suitable for PV- or wind-led operation. Residential heating and cooling by means of a compression heat pump (HP) system in connection with a thermal storage constitute a prototypical case to apply and develop a load shifting strategy. Extending the system with a PV plant increases the scope also in the direction of power generation. Such a system poses an interesting prototype for detailed investigation of demand-side but also (renewable) electricity generation related aspects. The PhD thesis of Pichler [3] includes more details.

2. Literature Review

As important research in this context, the work of Wimmer [4] has been identified. Wimmer investigated different model predictive control (MPC) approaches for residential heating, based on the preliminary work of Reiner [5]. In [4] the compressor speed is constant and a variation of the heat pump power over time is realized by means of pulse width modulation (PWM). That is, given a constant period between 0.4 h and 3.2 h, the on-time of the heat pump is varied to adjusted the average heating power over this period. Wimmer analyzed building models of different complexity from 2nd to 4th order. Although, *solar radiation* as internal building load was found to intensively interfere with the building and the room temperature, it was *neglected* in [4]. Annual simulations have shown cost savings up to 13% -- compared to a standard controller -- and an electricity consumption reduction up to 3.5%. Eventually, the simplest (least square optimization) of the three developed algorithms has been successfully employed in a real building. The author noted that any future application for other buildings would require an adaption of the used building model.

Based on Wimmer's research Bianchi [6] continued and investigated an *adaptive* MPC approach for the purpose of heating a single family house. The main contribution of Bianchi is the introduction of an identification mechanism, which automatically adjusts the building model parameters during real operation. This way, the MPC approach of Wimmer has been supplemented to be suitable for application in different single family houses. Principally, Bianchi's approach should allow for plug-and-play application of model predictive controlled heat pumps. However, no report on experience with real applications was found.

More recent research such as [7] deals with the topic demand side management (DSM) with heat pumps for single family houses with floor heating. In this article, a prediction horizon of 24 h has been found to outperform smaller prediction horizons in terms of renewable energy utilization with nearly negligible impact on the comfort.

3. Reference System and Methods

The investigated system in figure 1 comprises two active components: a compression HP and a PV plant, and two classical passive components: a thermal energy storage (TES) for DHW purpose and a thermally activated building system (TABS) as part of the single-family house. The HP, the TES and the TABS are connected through one hydronic system; electrical interconnections are not relevant for the analysis, although, the grid consumption and grid feed-ins are determined.

The special feature about the whole DSM idea in this context is the fact, that through suitably scheduled HP operation the classical passive TES and TABS may become pseudo active thermal components. A properly scheduled management reflects at the grid side with two main characteristics: first, damped electricity demand at times with thermal peak load, and second, limited feed-ins at times with high PV generation. This HP operation management is implemented by means of a model predictive controller (MPC).

Actually, the TABS considered is a common floor heating system on both floor levels of the single-family house. In addition to the principal thermal system, figure 1 indicates also the PV module area on the roof of the building. This PV area is located on the south facing roof, compare with figure 2. The HP – with its refrigerant cycle drawn

in figure 3 – is a ground source HP with speed controlled compressor. The main control tasks for this reference system refer to the room-air temperature (ϑ_{ra}) control and to the control of the temperature in the upper part of the TES (ϑ_{TES}). In the following only the heating case is discussed in detail.

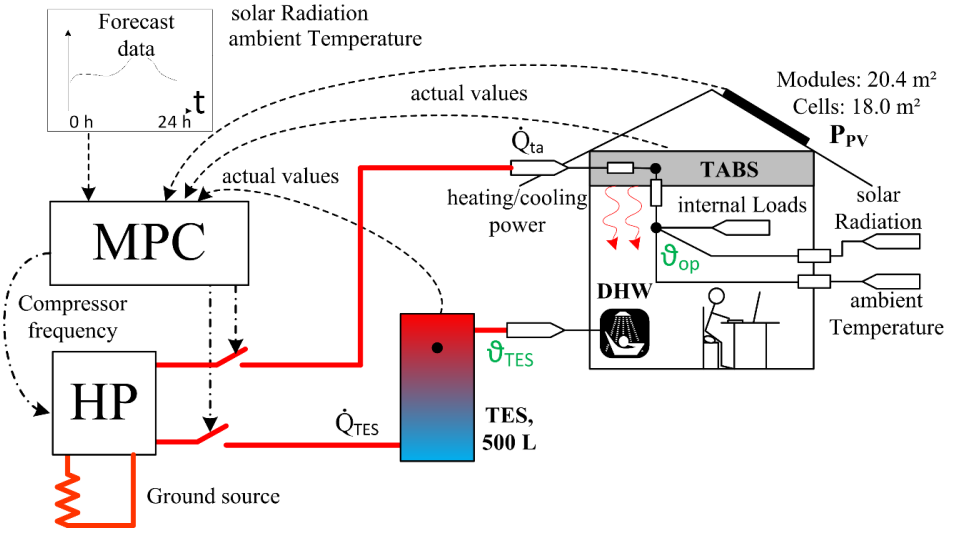


Fig. 1. Overview of the investigated system.

The complete reference system is set-up and simulated in TRNSYS [8]. The thermal building model including the TABS is implemented with TRNSYS type 56. The TES is a standard buffer storage (type 534). The complex TRNSYS simulation represents an analysis on a very detailed level, conducted with a time step of 2 min. In addition to the thermal building model, the hydronic cycle and the TES also the compression HP is modelled on a detailed level. For details on the hydronic circuit etc. the authors refer to the report of the closely related national project TheBat [9] or [3].

3.1. Thermal Storages and Building Model

The modelled single-family house depicted in figure 2 presents a state of the art building with a specific annual heating demand of approximately 45 kWh/m². For this research the building (model) originally defined in IEA SHC Task 44 [10] was slightly modified in terms of the heat emission system. In contrast to the original building, the actually investigated building uses the active layer option in type 56 to implement the TABS, cf. [11]. The DHW demand profile (2133 kWh/a) is based on the definitions made in SHC Task 44 (Report C1 Part A: Ch.6) [10]. However, the draw-off temperature for this research is limited to 50°C. In contrast to the original building definitions, internal building gains are neglected and hence the specific **annual** heating demand increases to 60 kWh/m², i.e. by approximately 15 kWh/m².

The thermal storages of the system are first, the TES, which is a simple buffer storage filled with 500 L plain water, and second, the thermal storage mass of the TABS. Activated is the 12 cm thick plaster in the 1st and the 2nd floor. Apart from this directly heated part of the building, the whole building construction represents an indirect thermal storage that also contributes to the thermal inertia of the building.

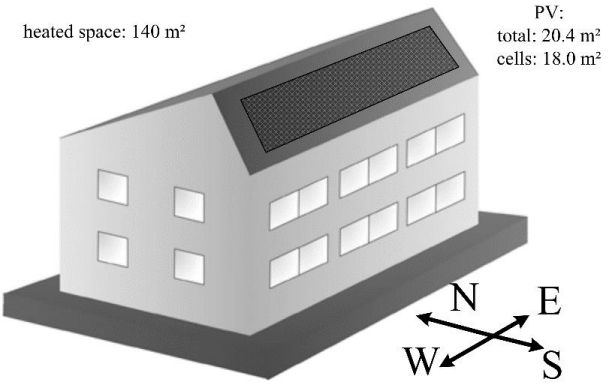


Fig. 2. Overview on the construction of the investigated building, modelled with TRNSYS, cf. [10].

3.2. Heat Pump and Operation Modes

The HP – with its refrigerant cycle and a typical temperature-enthalpy (ϑ-h) diagram drawn in figure 3 – is a ground source HP with speed controlled compressor. The main components are the evaporator (e), the scroll compressor, the desuperheater (d), the condenser (c) and the economizer (eco). The HP is modelled on a detailed level. For a description of the used model, see [12]. The applied HP parametrization is based on extensive validation with a real laboratory HP set-up [13]. However, a few heat exchanger parameters were adapted for this study, hence the overall absolute performance of the HP must not be directly compared to commercial products.

The size and performance of the HP are explained with the following technical data which hold for a compressor speed of 105 Hz: nominal heating capacity 9 kW(B0W35), at this stage the electrical consumption is $\mathrm{P_{comp}} = 2.6\,\mathrm{kW}$ and the thermal output through the condenser and the desuperheater are $\dot{\mathrm{Q}}_{\mathrm{cond}} = 6.73\,\mathrm{kW}$ and $\dot{\mathrm{Q}}_{\mathrm{desup}} = 2.27\,\mathrm{kW}$.

The compressor operating limits are generally given in terms of polygons in a 2D diagram, with x being the evaporating temperature and y being the condensing temperature. The area inside the drawn polygons show the possible operating range as a function of evaporating- and condensing-temperature. Given the relevant range of the source (brine) temperature (3 °C – 15 °C, obtained with Kasuda($z = -2\ m$) $- 4\ K$, compare with [14]) and a required desuperheater outlet temperature of 50 °C for (DHW) TES heating, the possible operating range is from 30 Hz to approximately 110 Hz.

Section 3.4 explains the implementation of the HP characteristics in the MPC controller model. For this research, it is based on extensive simulations and approximation of relevant physical relations through polynomial functions. Concerning practical applications, HP manufacturer specifications may replace the extensive simulations.

Two operation modes must be distinguished for the HP. The first mode relates to *space heating* via the TABS, and is termed TABS-mode. The second operation mode relates to the *TES heating* and is termed TES-mode. During TES-mode the condenser and the desuperheater mass flow rate are the same, and the HP outlet is directly supplied at the top of the TES. The HP outlet set temperature is 50 °C during TES-mode. In TABS-mode, which is the case for figure 3, the HP operates with $\Delta T_{cond} = 5\ K$ at the water side (w1 – w2) and a small share of the water flow rate is supplied to the desuperheater and heated up to 50 °C (d1 – d2).

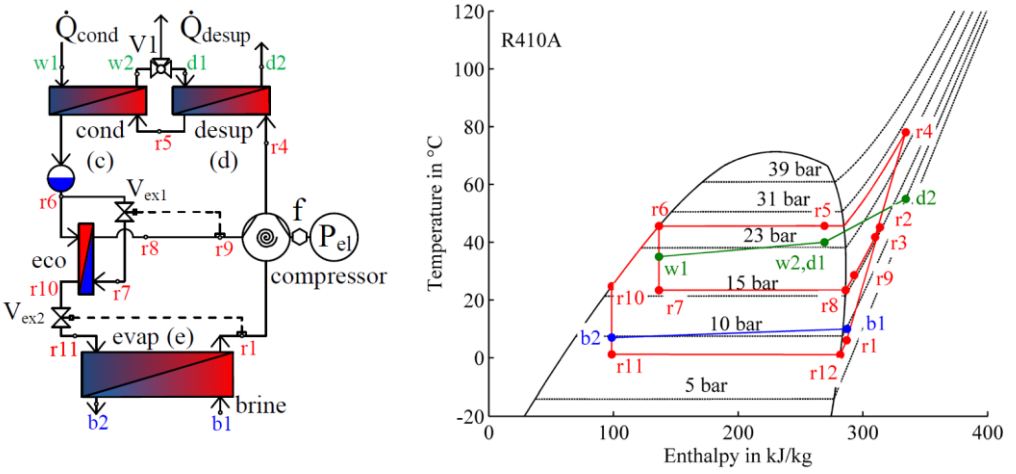


Fig. 3. Heat Pump Refrigerant Cycle and typical Temperature-Enthalpy-diagram.

3.3. Simulation Boundary Conditions

All presented results refer to annual simulation results. Used weather data within the simulation are synthetic METEONORM 7 [15] data for the location Innsbruck University, Austria; the temperatures are based on the data period: 2000-2009 and the solar irradiance is based on the data period: 1986-2005. The TRNSYS simulation time step is 2 min. The PV model is based on the 4-parameter approach developed by Eckstein [16] with the assumptions $\tau\alpha = 0.85$ (optical transmission absorption product) and $\eta_{converter} = 0.94$.

The DHW provision requirements and the desired room air temperature (ϑ_{ra}) range (set between 22 °C and 26 °C) indirectly define the required temperatures of the TES (ϑ_{TES}) and the TABS (ϑ_{TABS}). The DHW is prepared through a fresh water station taking thermal energy from the top part of the TES, which is heated up to 50 °C. The total annual DHW demand is 2133 kWh. As stated above, internal building gains are neglected in this study. The HP operation for the *base case scenario* corresponds to a simple control of the return temperature according to the ambient temperature. In this case the HP compressor frequency is adjusted linearly as a function of the ambient temperature.

3.4. Model Predictive Controller

The main control tasks refer to the room-air temperature (ϑ_{ra}) control and to the control of the temperature in the upper part of the TES (ϑ_{TES}) – both temperatures must be kept within a certain bandwidth. This research considers only space heating but no cooling. The selected MPC approach is based on two separate MPC's with higher priority given to the one controlling the TES. According to the HP operation modes the two MPC's are termed TABS-MPC and TES-MPC; *only the TABS-MPC is explained in the following*.

Figure 4 illustrates the most important elements of the MPC scheme. The basic MPC ingredients are *prediction data*, a *dynamic model* (building model) and a suitable *cost function*. In terms of data and parameters, one requires the prediction data (weather forecast), actual sensor data (room temperature), different reference values (set temperatures and limits) and numerous cost function parameters. The overall control task of the TABS-MPC is to sustain the room temperature between 20 °C and 26 °C. The MPC scheme is implemented in MATLAB [17] making use of YALMIP [18].

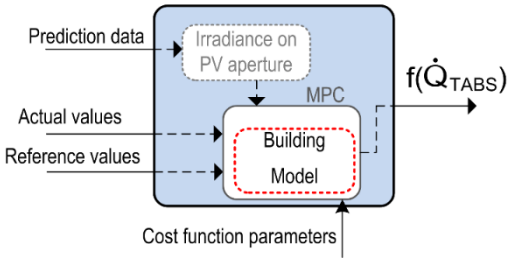


Fig. 4. Overview on model predictive control scheme for space heating (MPC-TABS).

The employed building model is physically motivated, but the estimated model parameters are a mixture of physical and lumped physical parameters. In the following, the building model, which is a state space model of 4th order, is simply abbreviated as $\vartheta_{op,i} = \mathcal{M}(\dot{Q}_{ta,i}, \dots)$, that is, the operative room temperature as a function of the thermal energy flux supplied to the TABS and numerous external variables (solar radiation, ambient temperature, etc.) which are indicated by the dots.

The actual thermal heat flux supplied to the TABS of the building ($\dot{Q}_{ta}$ cf. figure 1) is determined by means of repeated minimization of the following cost function:

$$\min_{\dot{\mathbf{Q}}_{ta}, \mathbf{s}, \Delta\mathbf{T}} J(\dot{\mathbf{Q}}_{ta}, \mathbf{s}, \Delta\mathbf{T}) = \sum_i \underbrace{R_{u,i} \left|\dot{Q}_{ta,i}\right|}_{Energy} + \underbrace{R_{s,i} \left|s_i\right|^2}_{Tracking} + \underbrace{R_T \left|\Delta T_{i+1}\right|^2}_{therm.Comfort} \tag{1}$$

subject to

$$\begin{aligned}
&\vartheta_{air,1}, \vartheta_{air,2}, \vartheta_{ta} \text{ given from measurements (TRNSYS simulation)} \\
&\vartheta_{op,i+1} := \mathcal{M}(\dot{Q}_{ta,i}, \dots) \\
&\dot{Q}_{ta,min} \le \dot{Q}_{ta,i} \le \dot{Q}_{ta,max}, \qquad 0 \le \dot{Q}_{ta,min} \\
&\dot{Q}^L_{ta,ref,i} - s_i \le \dot{Q}_{ta,i} \le \dot{Q}_{ta,ref,i} + s_i, \quad 0 \le s_i \\
&\vartheta_{op,min} - \Delta T_{i+1} \le \vartheta_{op,i+1} \le \vartheta_{op,max} + \Delta T_{i+1}, \quad 0 \le \Delta T_{i+1}
\end{aligned}$$

The value of the cost function $J(\dots)$ describes the optimization-related costs. An optimization program strives to minimize these costs through variation of the variable $\dot{Q}_{ta,i}$; the variables s (the tracking term slack variable) and ΔT (the slack variable indicating a comfort violation) give some additional freedom to the optimizer. The cost function consists of three terms: the energy term which considers the real energy price through the weight $R_{u,i}$, the tracking term with weight $R_{s,i}$, and the thermal comfort term with the weight R_T. Through the three weights, it is possible to adjust the importance of each aspect during the optimization. The most important constraint to understand PV tracking is the penultimate inequality in (1). The reference value expression $\dot{Q}_{ta,ref,i}$ is a function of the (predicted) generated PV power and the (predicted) HP condenser inlet temperature $\approx\vartheta_{ta}$. If the PV power goes beyond a specific value then $Q^L_{ta,ref,i} = Q_{ta,ref,i}$ which means that $\dot{Q}_{ta,i}$ is more or less fixed or clamped; deviation is only possible with $s_i > 0$, hence only the slack variable s_i can relax this constraint which increases the costs. The smaller s_i the closer is the electrical power demand of the HP to the PV generation. The derivation of this *reference value expression* requires the HP characteristic function $\dot{Q}_{cond}(P_{el}, \vartheta_{ci})$. Extensive simulations led to this function for this research, in practice it may be obtained from lab measurements of the HP manufacturer. The variable ΔT_{i+1} indicates the comfort violation, the smaller this value the smaller the comfort term in the cost function.

4. Results

Table 1 provides a summary for all relevant external variables of the simulation on a monthly basis. The most important variables are the outside ambient temperature (ϑ_{oa}) and the total horizontal solar radiation ($H_{tot,hor}$) in the fourth column. The ground temperature (ϑ_{grd}) refers to the temperature for calculation of the building losses against ground. The last three columns provide details on the PV-System. H_{PV} is the specific energy radiated onto the PV surface area, W_{PV} provides the PV yield and ϑ_{cell} is the cell temperature during PV operation.

Table 1. Summary of external variable values on a monthly basis – mean values and standard deviation (weather data Innsbruck).

	ϑ_{oa} ° C	RH_{oa} %	ϑ_{grd} ° C	$H_{tot,hor}$ kWh/m^2	H_{PV} kWh/m^2	W_{PV} kWh/m^2	$\vartheta_{cell,>15W}$ ° C
Jan	-1.8 ± 4.8	83.8 ± 11.8	0.3 ± 0.2	45.5	99.3	12.5	10.0 ± 7.4
Feb	0.9 ± 4.7	78.2 ± 14.0	0.8 ± 0.5	64.0	105.6	13.1	11.8 ± 7.5
Mar	5.1 ± 5.3	73.9 ± 17.5	3.5 ± 1.1	108.3	145.7	17.6	17.8 ± 8.1
Apr	9.8 ± 5.4	70.0 ± 18.8	7.7 ± 1.3	135.0	147.7	17.5	21.9 ± 8.7
May	15.1 ± 5.4	69.3 ± 20.0	12.4 ± 1.3	172.2	159.8	18.5	27.2 ± 8.5
Jun	17.4 ± 5.2	72.7 ± 18.3	16.2 ± 0.9	172.5	150.9	17.3	28.6 ± 8.0
Jul	18.5 ± 5.0	72.9 ± 18.8	18.1 ± 0.3	176.1	159.4	18.2	29.8 ± 7.8
Aug	18.2 ± 4.7	74.5 ± 16.6	17.7 ± 0.5	148.1	150.6	17.3	29.9 ± 7.5
Sep	13.8 ± 4.6	77.9 ± 15.0	14.9 ± 1.1	111.8	135.8	15.9	25.4 ± 7.3
Oct	9.9 ± 4.8	80.0 ± 14.5	10.6 ± 1.4	81.6	126.1	15.1	21.4 ± 7.1
Nov	3.9 ± 4.3	82.9 ± 12.0	6.0 ± 1.3	45.4	82.0	10.1	13.3 ± 6.7
Dec	-0.4 ± 4.4	84.4 ± 11.5	2.2 ± 0.9	35.5	80.1	10.1	9.4 ± 6.5
annual	9.2 ± 8.7	76.7 ± 16.8	9.2 ± 6.5	1296.1	1542.8	183.3	20.5 ± 7.6

Figure 5 shows simulation results for a typical week in winter. The top graph shows the trajectory for the top storage temperature (ϑ_{TES}) the operative room air temperature (ϑ_{op}) and the average (first and second floor) temperature for the TABS (ϑ_{ta}). The middle graph shows the heat inputs for the TES and the TABS, and the lowest graph shows the outside ambient temperature (ϑ_{oa}), the PV power (P_{PV}) and the HP compressor power consumption (P_{comp}).

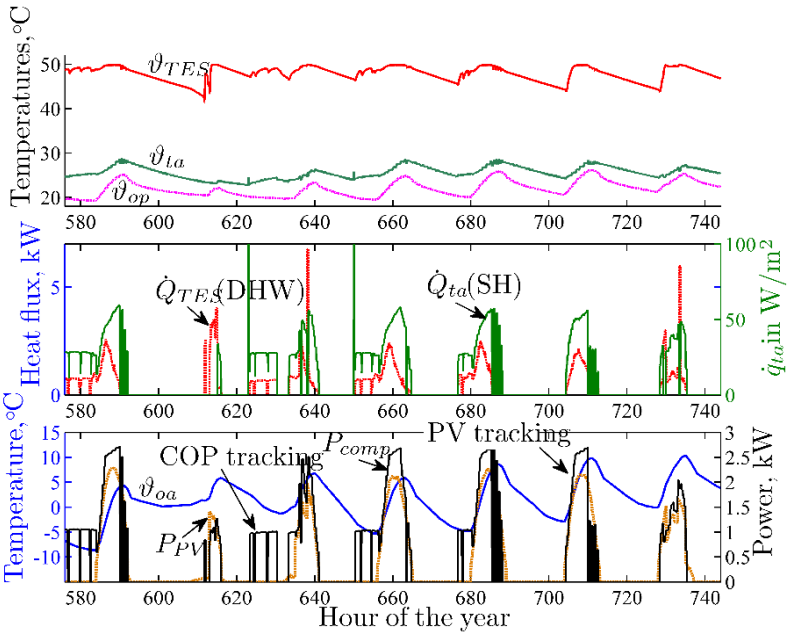


Fig. 5. MPC in winter, typical trajectories for temperatures and heat fluxes over a week. $\dot{Q}_{ta}$ left or right scale, $\dot{Q}_{TES}$ only left scale.

The overall goal is to operate the HP in such a way that as much PV energy as possible is used for its operation, which is clearly demonstrated in the bottom graph. At the PV maximum, the electrical power consumption of the HP tends to be a few 100 W above the PV generation; the explanation is an inaccurate PV power forecast within the MPC framework (simpler model compared to the TRNSYS simulation). The frequent on/off switching for decreasing PV power is the result of reaching the upper comfort limit in the building (26 °C) and the upper temperature limit in the storage (50 °C). The relatively high upper comfort limit for the building allows a maximum utilization of the PV energy, although the 26 °C rarely occur and if at all, then only over a very short time (< 2 h). If the PV power is zero, the HP switches on only to prevent comfort violations.

The temperatures in the top graph show a clear pattern as a result of the PV-led HP operation. Both, the TABS and the TES achieve a minimum temperature just before the solar radiation increases. This characteristic is plausible and directly in line with the original idea of exploitation of thermal heat storage capacities. With all thermal storage capacities being at the lowest possible temperatures prior to PV availability, a maximum of PV power can be converted to heat (by means of the HP) and temporary "stored". During the heating phase (in winter), there is hardly any activation of the HP for pure TES heating (HP operation for SH purposes includes always TES heating through the desuperheater at 50 °C with low power, which is not shown in Fig.1). The red peaks in the middle graph indicate pure TES heating. A similar picture holds for summer, but since there is no space heating demand, the PV-led operating phase is relatively short, compared to Fig. 5.

4.1. Energy Balance and Energy Flows

Figure 6 shows the total energy flows. Due to the absence of internal building gains (which are not considered for this study), the heating demand is relatively high (8972 kWh) compared to the results in [10].

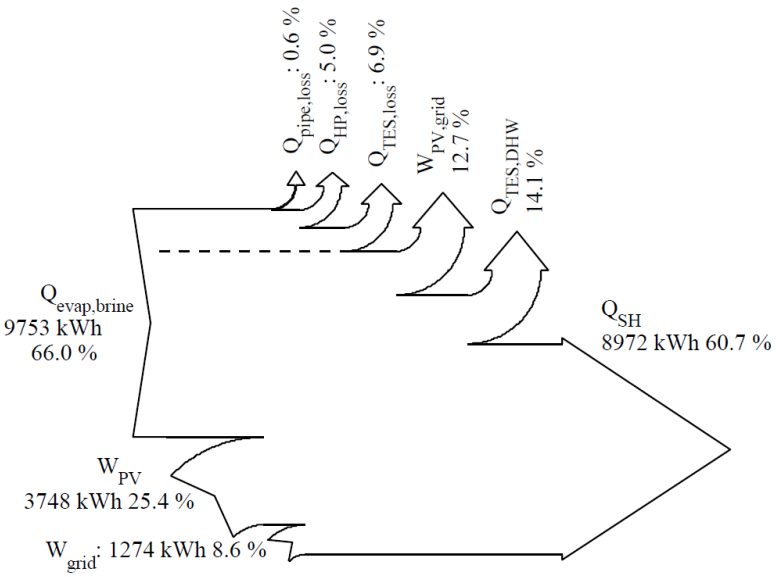


Fig. 6. Overview total annual energy amounts MPC operation -- V1.3a in [3].

The three flow diagrams in figure 7 give an overview of the total electrical energies (left), the distribution of the generated PV energy split according to use (center), and the origin of the actual electricity consumption of the HP. The grid electricity demand of 1274 kWh is compared to the base case without MPC (2467 kWh see figure 8) relatively low.

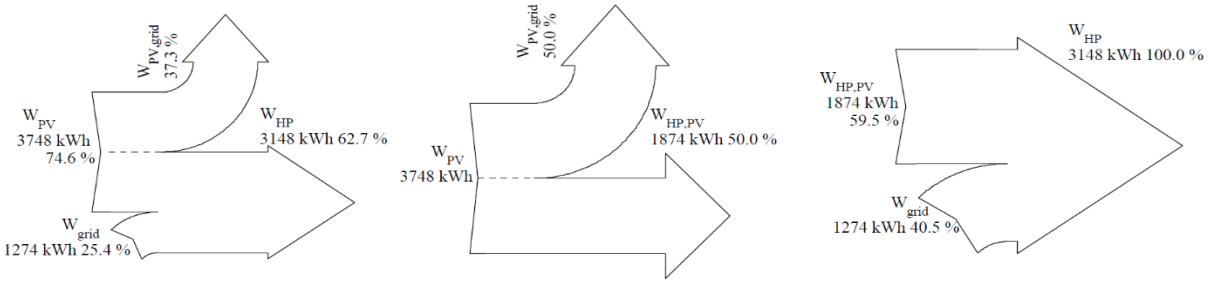


Fig. 7. Electrical energies: Overview (left), PV generated energy split according to use (middle) and heat pump electrical consumption split according to electricity origin (right) – MPC scenario V1.3a in [3].

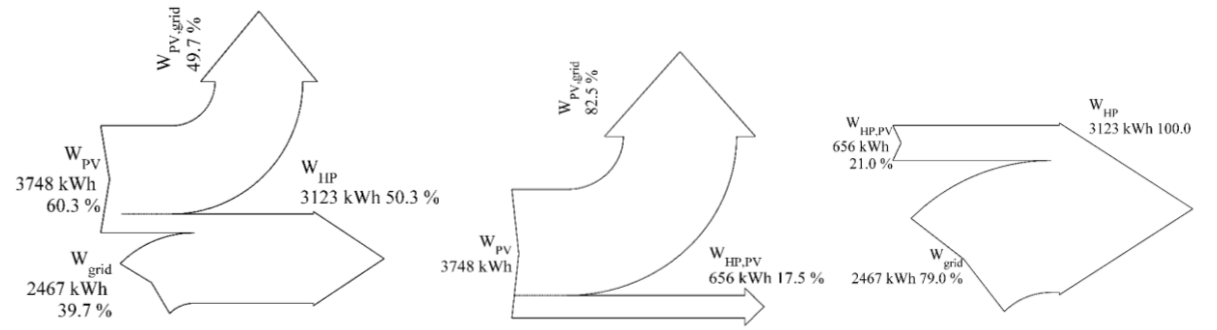


Fig. 8. Electrical energies: Overview (left), PV generated energy split according to use (middle) and heat pump electrical consumption split according to electricity origin (right) – Base Case scenario V0.1 in [3].

The HP directly consumes 50% of the generated PV energy in course of one year – for the base case this share is approximately 20% based only on coincidence. A detailed analysis shows that the heating season from October to April achieves a PV self-consumption of 84%. The electricity consumed by the HP in the course of one year consists of approximately 60% of PV electricity and 40% of grid electricity – for the base case the shares are approximately 24% and 76%.

The internal building gains are neglected in the present simulation results. On the one hand, this increases the potential PV consumption of the HP. However, at the same time the electrical energy flows were analyzed without taking into account household electricity consumption. If an average household electricity consumption of 3500 kWh is assumed and considered as internal gains, a rough conservative estimate still results in a further increase of 13 percentage points of PV self-consumption.

4.2. Heat pump efficiency

In principle, a PV-led and an efficient operation of the HP are contradictory. The reason is: in PV-led operation the HP is operated in a way, that the (compressor) power demand corresponds to the current PV generation. In order to achieve this, the compressor speed is varied within the possible range, and within this range there are, of course, operating points that are efficient and others that are less efficient. If there is no PV generation, the HP operates with maximum efficiency if possible. For the MPC scenario, the achieved seasonal performance factor (SPF) -- calculated by means of the heat provided at the condenser and the desuperheater, and the total electrical

power consumption of the HP (compressor, electronics, circulation pump for condenser and desuperheater) – is 3.72. For the entire system (SPFsys) – from the useful energies and the total power consumption – one obtains 3.32. The according values for the base case scenario are SPF=3.95 and SPFsys=3.55. That is, the SPF for PV-led HP operation decreases by approximately 5% compared to the base case scenario. However, the grid consumption and the economic costs decrease. To evaluate the performance of the MPC approach in terms of PV-tracking an SPF_{ctr} -- calculated by means of the heat provided at the condenser and the desuperheater, and the total electrical power consumption of the HP from the grid – is defined. For the MPC scenario it is 9.6.

4.3. Heat pump efficiency tracking

If the PV-led operation is switched off during the whole simulation and instead an efficiency tracking is implemented via the cost function in equation 1 the SPF increases to 4.13 and the SPFsys increases to 3.68. To this end the function $\dot{Q}_{ta,ref}$ must be replaced by a suitable alternative. HP operation with maximum efficiency may be not possible if a predicted comfort violation arises, in such case even during efficiency tracking the HP may operate at maximum compressor speed to maintain the required thermal output. That is, HP operation in efficiency tracking mode increases the SPF by 10% compared to the PV-led HP operation. For more details, see [3].

5. Summary and Conclusion

The end-consumer electricity price in Austria is **approximately** 20 cent/kWh and the grid feed-in remuneration for household generated photovoltaic (PV) energy is without any subsidies only 6 cent/kWh. This aspect and wishes from a demand-side-management point of view with respect to HP- and PV-operation are the main motivation for this research. This paper introduces and presents a holistic control approach for a compression heat pump in connection with a PV system for a single-family house. A model predictive control was developed and investigated by means of TRNSYS simulations.

The simulated PV system with an approximate size of 20 m² generates 3748 kWh electricity on an annual base. With the developed control approach the direct consumption of PV energy by the HP may be increased from 20% (base case scenario) to 50%. In winter, this number is even higher. The electrical energy consumed by the HP in the course of one year originates to a degree of approximately 60% from the PV in situ and 40% are consumed from the grid – for the base case this shares are approximately 24% and 76%, respectively. Due to the wide range of compressor frequencies in PV-led HP operation mode the SPF for the MPC scenario is approximately 5 % below that of the base case scenario. Switching off the PV-led operation and applying instead a HP efficiency tracking with the same control approach, the SPF increases by 10% with respect to the PV-led HP operation or 5% with respect to the base case scenario.

The suggested control approach is viable to damp the HP electricity demand at times with normally high thermal peak load and it clearly reduces the feed-ins at times with high PV generation. In addition to the load shifting, the approach may be parametrized in such a way to maximize the HP efficiency during heating operation. Overall, the presented approach is very versatile. The obtained results may be utilized to derive simplified predictive rule based controllers but also for other calculations in various research scenarios, where the PV self-consumption is relevant. Finally, the concept is likely to be implemented in one or the other version in future heat pumps.

Acknowledgements

The project "The thermal battery in the smart grid in combination with heat pumps – an interaction optimization (TheBat)" is sponsored by the Austrian Climate and Energy Fund and conducted within the framework of the program „ENERGY MISSION AUSTRIA" (FFG-Project-Number 838657). The project IEA HPP Annex 42 „Heat pumps in smart energy grids' for sustainable cities" is conducted within the framework of the IEA-collaboration on behalf of the Austrian Ministry for Transport, Innovation and Technology (FFG-Project-Number 848119).

References

[1] P. Biermayr, M. Eberl, M. Enigl, H. Fechner, C. Kristöfel, K. Leonhartsberger, F. Maringer, S. Moidl, C. Schmidl, C. Strasser, W. Weiss, and E. Wopienka, "Innovative Energietechnologien in Österreich," Bundesministerium für Verkehr, Innovation und Technologie, Tech. Rep., 2016.

[2] A. Schaefer, H. Schuster, U. Kasper, and A. Moser, *Electrochemical Energy Storage for Renewable Sources and Grid Balancing – Ch.3*, P. T. Mosely and J. Garche, Eds. Elsevier, 2015.

[3] M. F. Pichler, "MODEL PREDICTIVE CONTROL FOR HEATING IN RESIDENTIAL BUILDINGS – PV-led heat pump operation in a single family house," Ph.D. thesis , Graz University of Technology, 2016, draft version.

[4] R. W. Wimmer, "Regelung einer Waermepumpenanlage mit Model Predictive Control," Ph.D. dissertation, ETH Zuerich, 2004.

[5] G. Reiner, E. Shafai, R. Wimmer, D. Zogg, H. Gabathuler, H. Mayer, and H. Bruderer, "Kurztestmethode fuer Warmepumpenanlagen. Phase 1 bis 3: Messung, Modellierung und Erprobung der Parameteridentifikation." Forschungsprogramm UAW des Bundesamtes fuer Energie, Bern, Tech. Rep., 1998.

[6] M. A. Bianchi, "Adaptive Modellbasierte Praediktive Regelung einer Kleinwaermepumpenanlage," Ph.D. dissertation, ETH Zuerich, 2006.

[7] J. Y. Young, "DEMAND-SIDE-MANAGEMENT WITH HEAT PUMPS FOR SINGLE FAMILY HOUSES," *Proceedings of BS2013, 13th Conference of International Building Performance Simulation Association, Chambery, France*, August 2013.

[8] S. Klein, W. Beckman, J. Mitchell, J. Duffie, N. Duffie, T. Freeman, J. Mitchell, J. Braun, B. Evans, J. Kummer, R. Urban, A. Fiksel, J. Thornton, N. Blair, P. Williams, D. Bradley, T. McDowell, M. Kummert, D. Arias, and M. Duffy, *A TRaNsient SYstems Simulation Program – TRNSYS 17.00.0019, Manual*, Solar Energy Laboratory, University of Wisconsin-Madison, 2010. [Online]. Available: http://sel.me.wisc.edu/trnsys

[9] M. F. Pichler, A.Heinz and R. Rieberer, "TheBat – Die Thermische Batterie im Smart Grid in Kombination mit WÃ¤rmepumpen – eine Interaktionsoptimierung," Graz University of Technology, Tech. Rep., 2016.

[10] R. Dott, M. Y. Haller, J. Ruschenburg, F. Ochs, and J. Bony, "The Reference Framework for System Simulations of the IEA SHC Task 44 / HPP Annex 38 Part A: General Simulation Boundary Conditions; Part B: Buildings and Space Heat Load," IEA, Tech. Rep., 2013.

[11] M. Koschenz and B. Lehmann, *Thermoaktive Bauteilsysteme TABS*, M. Koschenz, Ed. EMPA, 2000.

[12] R. Dott, T. Afjei, A. Dalibard, D. Carbonell, A. Heinz, M. Haller, and A. Witzig, "Models of Sub-components and Validation for the IEA SHC Task 44/HPP Annex 38, Part C: Heat Pump Models, A Technical Report of Sub-task C, Deliverable C2.1 Part C," Tech. Rep., 2012.

[13] F. Hengel, A. Heinz, and R. Rieberer, "Performance analysis of a heat pump with desuperheater for residential buildings using different control and implementation strategies," *Applied Thermal Engineering*, vol. 105, pp. 256 – 265, 2016. [Online]. Available: http://www.sciencedirect.com/science/article/pii/S1359431116307785

[14] T. Kasuda and P. Archenbach, "Earth Temperature and Thermal Diffusivity at Selected Stations in the United States," *ASHRAE Transactions*, vol. 71, p. Part 1, 1965.

[15] Meteonorm 7.0.21.5, Global Meteorological Database for Engineers, Planners and Education, Software and Data on CD-ROM. Meteotest, Bern, Switzerland, 2013.

[16] J. H. Eckstein, "Detailed modelling of photovoltaic system components," Master's thesis, University of Wisconsin - Madison, 1990.

[17] T. M. GmbH, *MATLAB R2013b*, 2013.

[18] J. Löfberg, "YALMIP : A Toolbox for Modeling and Optimization in MATLAB," in *In Proceedings of the CACSD Conference, Taipei, Taiwan*, 2004.